

MEMORANDUM REPORT BRL-MR-3782

BRL

DESIGN AND FINITE-ELEMENT ANALYSIS
OF A SABOT FOR A 60MM FLARED RAMJET

RAYMOND VON WAHLDE

DTIC
ELECTE
OCT 12 1989
S B D

OCTOBER 1989

APPROVED FOR PUBLIC RELEASE; DISTRIBUTION UNLIMITED.

U.S. ARMY LABORATORY COMMAND

BALLISTIC RESEARCH LABORATORY
ABERDEEN PROVING GROUND, MARYLAND

AD-A213 271

DESTRUCTION NOTICE

Destroy this report when it is no longer needed. DO NOT return it to the originator.

Additional copies of this report may be obtained from the National Technical Information Service, U.S. Department of Commerce, Springfield, VA 22161.

The findings of this report are not to be construed as an official Department of the Army position, unless so designated by other authorized documents.

The use of trade names or manufacturers' names in this report does not constitute indorsement of any commercial product.

REPORT DOCUMENTATION PAGE

Form Approved
OMB No. 0704-0188

1a. REPORT SECURITY CLASSIFICATION UNCLASSIFIED		1b. RESTRICTIVE MARKINGS	
2a. SECURITY CLASSIFICATION AUTHORITY		3. DISTRIBUTION/AVAILABILITY OF REPORT Approved for public release; distribution is unlimited.	
2b. DECLASSIFICATION/DOWNGRADING SCHEDULE			
4. PERFORMING ORGANIZATION REPORT NUMBER(S) BRL-MR-3782		5. MONITORING ORGANIZATION REPORT NUMBER(S)	
6a. NAME OF PERFORMING ORGANIZATION U.S. Army Ballistic Research Laboratory	6b. OFFICE SYMBOL (If applicable) SLCBR-LF	7a. NAME OF MONITORING ORGANIZATION	
6c. ADDRESS (City, State, and ZIP Code) Aberdeen Proving Ground, MD 21005-5066		7b. ADDRESS (City, State, and ZIP Code)	
8a. NAME OF FUNDING/SPONSORING ORGANIZATION U.S. Army Ballistic Research Laboratory	8b. OFFICE SYMBOL (If applicable) SLCBR-DD-T	9. PROCUREMENT INSTRUMENT IDENTIFICATION NUMBER	
8c. ADDRESS (City, State, and ZIP Code) Aberdeen Proving Ground, MD 21005-5066		10. SOURCE OF FUNDING NUMBERS	
		PROGRAM ELEMENT NO. 62618A	PROJECT NO. 1L1 62618AHB0
		TASK NO.	WORK UNIT ACCESSION NO.
11. TITLE (Include Security Classification) Design and Finite-Element Analysis of a Sabot for a 60mm Flared Ramjet			
12. PERSONAL AUTHOR(S) Raymond Von Wahlde			
13a. TYPE OF REPORT Memorandum Report	13b. TIME COVERED FROM _____ TO _____	14. DATE OF REPORT (Year, Month, Day)	15. PAGE COUNT
16. SUPPLEMENTARY NOTATION			
17. COSATI CODES		18. SUBJECT TERMS (Continue on reverse if necessary and identify by block number)	
FIELD	GROUP	SUB-GROUP	
13	13		
19	10		
		Finite-Element Sabot von Mises Stress Yield Stress Ramjet	
19. ABSTRACT (Continue on reverse if necessary and identify by block number) This report details the design process and finite-element analysis of a sabot package for a 60mm flared ramjet to be fired from a 105mm gun for a spin test program.			
20. DISTRIBUTION/AVAILABILITY OF ABSTRACT <input type="checkbox"/> UNCLASSIFIED/UNLIMITED <input checked="" type="checkbox"/> SAME AS RPT. <input type="checkbox"/> DTIC USERS		21. ABSTRACT SECURITY CLASSIFICATION UNCLASSIFIED	
22a. NAME OF RESPONSIBLE INDIVIDUAL Raymond Von Wahlde		22b. TELEPHONE (Include Area Code) (301)-278-4680	22c. OFFICE SYMBOL SLCBR-LF-A

Table of Contents

	<u>Page</u>
List of Figures	v
I. Introduction	1
II. Initial Design of the Sabot Package	1
III. Loading Conditions	2
1. Axial Acceleration	2
2. Angular Acceleration	3
3. Lateral Acceleration	3
4. Sabot Engraving Force	3
5. Torque load on the pre-engraved rifling	4
6. Summary	4
IV. Initial Design Analysis	4
1. Sabot Petals	5
2. Pusher	6
3. Pre-Engraved Rifling	6
4. Pusher Extension	7
V. Structural Integrity Test	7
VI. Design Modifications	8
1. Sabot Petals	8
2. Steel Boreriders	9
3. Copper Rotating Band	9
a. Shrink Fit	9
b. Engraving Force	10
VII. Summary and Conclusions	11
References	19
List of Symbols	21
Distribution List	23

List of Figures

<u>Figure</u>		<u>Page</u>
1	Basic Solid Fuel Ramjet (SFRJ).	12
2	60mm flared ramjet sabot package.	12
3	Spin driving mechanism.	13
4	Finite-Element (FE) model mesh.	13
5	Sabot petal stress contours.	14
6	Pusher stress contours.	14
7	Rifling engagement.	15
8	Pre-engraved rifling FE model.	15
9	Pusher extension stress.	16
10	Modifications to sabot package.	16
11	Unrestrained sabot borerider FE model.	17
12	Restrained sabot borerider FE model.	17
13	Rotating band FE model.	18

Accession For	
NTIS GRA&I	<input checked="" type="checkbox"/>
DTIC TAB	<input type="checkbox"/>
Unannounced	<input type="checkbox"/>
Justification	
By	
Distribution/	
Availability Codes	
Dist	Avail and/or Special
A-1	



I. Introduction

A basic solid-fuel ramjet (SFRJ) projectile is shown in Figure 1. A ramjet motor consisting of an inlet, hydrocarbon fuel and composite nozzle is housed in a hollow steel case. In flight, air is forced through the inlet, burns with the fuel, accelerates out the nozzle, and thus produces thrust.

The Chemical Systems Division of United Technologies Corporation (UTC), through tests done in conjunction with the Ballistic Research Laboratory (BRL), discovered that the rate at which the fuel regressed, i.e. the burn rate, was affected by the spin rate of the SFRJ. Higher spin causes a slower regression rate and hence less thrust.

In order to quantify this effect, UTC and BRL developed a program to flight-test a flare-stabilized SFRJ at four different spin rates. Four 105mm M68 gun tubes are to be utilized: the standard twist (one revolution in eighteen calibers, one-in-18), and three specially made tubes: a smooth bore, a one-in-12 and a one-in-25 twist.

This report details the design and finite-element analysis of a sabot package for the 60mm flared ramjet to be utilized in the spin test program. Also included are the results from the initial structural integrity flight-test, and the necessary design modifications.

II. Initial Design of the Sabot Package

The design process was an iterative one. First, the basic geometry of the sabot package needed to be determined. The function of each sabot component and the geometry of the ramjet dictated this. The second step was to determine, by simple calculations, the loading conditions on each component. In most cases these estimates were increased by a factor of 1.25 to allow for a safety margin. The next step was to create a Finite-Element (FE) model and analyze it using either SUPERSAP² or SUPERTAB.³ The resulting von Mises stress contours were compared to the yield strength of the component material to see if the piece would fail or not. Von Mises stress is determined by an empirical equation utilizing the components of stress in a material which is in a three-dimensional state of stress.⁴ It has proven to be a successful failure criterion in finite-element analysis.⁵

Each component was examined individually and also included in the finite-element model of the total package. If changes were needed, the component and package were re-analyzed. Finally, a structural integrity test was fired, which turned up problems requiring several design modifications, and the process was repeated.

The first iteration of the sabot package is shown in Figure 2. The major components are:

- a 60mm Flared Ramjet made of T-250 grade maraging steel
- three sabot petals made of 7075-T6 aluminum
- a pusher made of 7075-T6 aluminum
- a pusher extension made of T-250 grade maraging steel

Recent work on the aerodynamics of a 60mm fin-stabilized ramjet suggests that its exterior driving grooves have a destabilizing effect.⁶ Because of this possible effect, UTC excluded sabot grooving from the flared ramjet design. This precluded the use of a sabot package in which a grooved projectile is pulled along by a grooved sabot.

The ramjet would be launched out of the gun by a pusher and pusher extension. This pusher assembly (Figure 3) must also serve to spin the ramjet. The pre-engraved rifling engages the gun tube rifling and torques the pusher. The spin is transferred to the pusher extension through four Woodruff keys. The pusher extension spins up the ramjet by means of a toothed engagement. The pusher extension is attached to the pusher by means of a bolt and washer not shown in Figure 3.

The sabot petals laterally support the ramjet in the bore. The thinnest possible petals were desired so that the largest possible flare diameter might be used in order to provide greater aerodynamic stability. The flare also supports the ramjet in the bore. Three, rather than four, petals were chosen to achieve a stiffer structural design.

III. Loading Conditions

The dominant loads are the gun gas pressure load, the launch mass inertial load and the centrifugal load. Other loads of importance are those resulting from the lateral acceleration, the engraving force on the sabot petals, and those resulting from the torque on the rifling grooves and on the pusher extension teeth. The sabot package must survive the worst case loading conditions, which occur at the highest desired velocity, $V_z=1554$ m/s, in the highest twist gun, one-in-12.

1. Axial Acceleration

The pressure and inertial load are related through Newton's second law:

$$F = ma_z = P_{base}A_{bore} \quad (1)$$

where:

- m = total launch mass
- a_z = axial acceleration of the launch mass
- P_{base} = base pressure on the projectile
- A_{bore} = bore area of the gun tube
- F = Force

The effective projectile base pressure is typically only about two-thirds of the maximum chamber pressure. Using the maximum chamber pressure as a design pressure would lead to overly conservative design requirements.⁷ A peak pressure of 352 MPa was predicted from earlier charge development for similar launch masses. Thus a design pressure of two-thirds of this value was chosen.

A mass properties program was used to obtain accurate mass and moment of inertia estimates for each component of the launch package.⁸ Equation (1) yields an acceleration of about 40,000 g's. A design acceleration of 50,000 g's was used to provide a safety factor.

2. Angular Acceleration

An estimate for the peak angular acceleration was computed in order to calculate the torque load on the pre-engraved rifling (Section III.5.) This occurs when using the highest twist gun, in which the projectile makes one revolution in 12 calibers. At the design velocity, the spin rate, ω , is about 7,850 rad/s. The angular acceleration, $\dot{\omega}$, is approximately $\frac{\Delta\omega}{\Delta t}$ where $\Delta t \approx \frac{V_x}{a_x}$. Rounding up, this yields an $\dot{\omega} \approx 2.5 \times 10^6$ rad/s².

3. Lateral Acceleration

Axial acceleration down a gun tube has a lateral component, a_x , due to the non-straightness of the tube. A typical lateral travel, Δx , is .8mm in 1 meter of axial travel, Δz , or $\frac{\Delta x}{\Delta z} = .0008$. For rectilinear motion with constant acceleration, an equation of motion can be obtained:⁹

$$\Delta z = \frac{1}{2}a_z(\Delta t)^2 \text{ and } \Delta x = \frac{1}{2}a_x(\Delta t)^2 \quad (2)$$

Thus:

$$\frac{\Delta x}{\Delta z} = \frac{a_x}{a_z} \quad (3)$$

$a_x = 40$ g's. A side load of 50 g's was used for added safety.

A peak value for lateral acceleration for a 120mm tank gun is between 300-500 g's.¹⁰ This occurs at the muzzle and is due to the whip of the barrel. Because this peak value for lateral acceleration occurs after the peak axial acceleration, 50 g's may be sufficient.

4. Sabot Engraving Force

As the launch package spins, the petals move radially outward and are restrained by the barrel wall. This centrifugal force acts as a bearing load on the outer surface. Because of the lands and grooves of the gun tube rifling, only about one-third of the petal surface area is available to carry the load. If this stress is great enough, the petals can yield into the rifling and become engraved.

For a particle in circular motion the centrifugal force, $F_{centrifugal}$, is:⁹

$$F_{centrifugal} = m \frac{V_r^2}{R_{cg}} \quad (4)$$

where:

m = the mass of one sabot petal

R_{cg} = the radial center of gravity for one sabot petal

and V_r is the angular velocity:

$$V_r = \omega R_{cg} \quad (5)$$

This provides an estimate of the engraving force on the sabot petals.

5. Torque load on the pre-engraved rifling

The loading on the rifling was estimated by finding the torque necessary to spin up the launch package:

$$I_{zz}\dot{\omega} = F_{driving}r \quad (6)$$

where:

- I_{zz} = axial moment of inertia of the launch package
- $F_{driving}$ = torque driving force = $P_{driving}A_{rifling} \times 28$
- $P_{driving}$ = driving pressure
- $A_{rifling}$ = driving area of one rifling land
- r = radial distance to rifling

6. Summary

The design conditions are summarized as follows:

- V_z = 1554 m/s
- a_z = 50,000 g's
- a_r = 50 g's
- P_{base} = 234 MPa
- ω = 7,850 rad/s
- $\dot{\omega}$ = 2.5×10^6 rad/s²
- $P_{driving}$ = 69 MPa (on rifling)

IV. Initial Design Analysis

Figure 4 shows the finite-element mesh used for the analysis. The model consisted of 716 2D-axisymmetric elements and 7 boundary elements, using 911 nodes. The mesh was intentionally finer in areas of greater interest, e.g. at the front and middle supports and the bottom half of the sabot petals. Although not load-bearing members, the flare and the inner components of the ramjet were included in the FE model in order to account for their weight in the inertial loads.

For 2D-axisymmetric elements, there are two degrees of freedom: radial and axial. The nodes on the outer surface of the sabot petals were fixed radially because they would be restrained by the barrel. Ideally the model should be unrestrained in the axial direction since it is free to move down the barrel. However, because the FE software is a static analysis, the model must be completely restrained in all degrees of freedom.² At least

one node must be fixed axially. Because the forces on the model (Section III.6) are not balanced, false stresses would arise in those elements with fixed nodes. This was avoided by using boundary elements to support the model at its base. Boundary elements act like ultra-stiff springs and allow the model to displace without overly stressing the model at their attachment points. Boundary elements also give the reaction force necessary to resist a load.

The sabot components shared nodes at certain locations so that stress would be carried across their points of contact, e.g. between the bottom of the sabot petals and the pusher and between the pusher extension and ramjet.

The supports on the petals, and the ramjet did not share nodes because the petals do not carry the inertial load of the ramjet. However, the petals do laterally support the ramjet, and this loading must be included. These lateral loads were obtained by fixing the ramjet with boundary elements at the points of contact and applying the centrifugal load. The resulting reaction forces were then applied as nodal loads on the supports and ramjet. Nodal loads along the taper at the base of the petals were similarly determined.

1. Sabot Petals

The first step in designing the sabot petals was to determine an acceptable thickness. This was accomplished by treating them as a solid-of-revolution rather than three separate pieces. This is a valid assumption because the gun barrel prevents the sabot petals from moving radially. Previous analyses have successfully demonstrated that the petals may be considered as an axisymmetric body during the launch cycle.⁵ This allows one to model the sabot petals using axisymmetric elements and to apply the theoretical formulas for a thin cylindrical tube. The critical stress at which column buckling occurs is:¹¹

$$S' = \frac{E}{\sqrt{3}\sqrt{1-\nu^2}} \frac{t}{R} \quad (7)$$

where:

- R = mean radius of the tube
- t = thickness of the tube
- E = Modulus of Elasticity
- ν = Poisson's Ratio

This equation is applicable for tube lengths $\gg 1.72\sqrt{Rt}$ and for $\frac{R}{t} > 10$. Tests indicate actual buckling strengths are 40%-60% of this theoretical value. Therefore, Equation (7) becomes:¹¹

$$S' \approx .3E \frac{t}{R} \quad (8)$$

It was anticipated that a light-weight composite material would be required for the thin sabot petals. This would have resulted in an expensive and time consuming manufacturing process. However, the yield stress of 7075-T6 aluminum, used for S' in Equation (8), showed that a 1.27mm thick petal of this material might suffice. But, because the petals were not a true solid tube, a thickness of 3.81mm was chosen as an added safety factor. The sabot petals were considered to be the most critical components of the sabot package and were therefore conservatively designed.

Stress analysis of the petals indicated that the stress reached a failure level near the pusher. For this reason the petal thickness was increased past the flare. Subsequent analysis showed that the additional bearing area reduced the stress at this critical point. The integrity of the front and middle supports also was verified under the previously determined lateral loads (Figure 5.)

In addition to Equation (4), the centrifugal force also was estimated by restraining the nodes on the outside surface of a sabot petal model with boundary elements and applying the centrifugal load. The resulting reaction forces were comparable to the computed value. Dividing this force by one-third the sabot petal surface area gave an estimate for the engraving stress on the petals.

Another method was to construct a 3D finite-element model of a sabot petal, fix the outside surface, apply the centrifugal load, and look at the resulting stress. Each method gave stress values well below the yield stress of the material. For this reason it was felt that the petals would not engage the rifling.

2. Pusher

The pusher, shown in Figures 2 and 3, serves several functions. It literally pushes the ramjet and sabot petals out of the gun. It engages the barrel's rifling and spins up the launch package. It also holds a 105mm rubber obturator. An obturator prevents gas leakage by corking the gun tube rifling. These tasks dictated the profile of the pusher. The cavity at the base of the pusher lessens its weight. The projection at the front serves to align and laterally support the pusher extension.

The stress contours in the pusher model are shown in Figure 6. A small area of high stress beneath the pusher extension is acceptable because the pusher is very thick there. Localized yielding would redistribute and relieve the concentrated stress. The model contains the inertial, centrifugal and pressure loads but not the torque load on the rifling. This latter load could not be modeled axisymmetrically and required a 3D model.

3. Pre-Engraved Rifling

The pre-engraved rifling must engage the 28 lands and grooves of the barrel rifling, as shown in Figure 7. Separate pushers were made for each gun twist.

A finite-element model was constructed by creating a 3D slice of one rifling land (Figure 8.) The boundary conditions on the 3D brick elements were such that the axial symmetry of the pusher was maintained yet the rifling land was free to displace circumferentially.

The driving pressure, obtained from Equation (6), was applied to the driving face of the rifling land. The stress shown in Figure 8, resulting from this torque loading, must be superimposed on the stress in Figure 6, resulting from the other loads. Although the

stress in the lands appears to exceed the yield stress of the material, this was considered acceptable because the bulk of the land is below the yield stress of the material. Again, localized yielding would redistribute and relieve the stress. Therefore, it was concluded that the rifling would not shear off under the torque load.

4. Pusher Extension

The pusher extension spins up the ramjet by means of the toothed engagement shown in Figure 3. The teeth are shallow and sloped to allow a clean disengagement. In free flight, the ram air pressure through the hollow ramjet forces the pusher/extension assembly away from the ramjet. For the rifled tubes, the spinning pusher/extension is gyroscopically stable and should fall straight back without hitting the ramjet flare. For the smooth bore, it is assumed that the assembly's inertia should keep it from yawing and interfering with the flare.

The number of driving teeth, N_{teeth} , necessary to fully spin up the ramjet was determined by using Equation (6) to calculate the torque needed to overcome the ramjet's inertia.

In this case:

I_{zz}	= axial moment of inertia of the ramjet
$F_{driving}$	= torque driving force = $P_{driving} A_{teeth}$
$P_{driving}$	= driving pressure
A_{teeth}	= driving area of teeth = $N_{teeth}(h)(d)$
r	= radial distance to the driving teeth
h	= height of the driving teeth
d	= depth of the driving teeth

Allowing the driving pressure to approach half the yield strength of the maraging steel ($P_{driving} = 862 \text{ MPa}$) yields a value of $N_{teeth}=16$. As an added safety factor, twenty teeth were used. Thus $P_{driving} = 689 \text{ MPa}$.

The teeth were analyzed utilizing plane stress elements (2D elements of specified thickness.)² The stress resulting from $P_{driving}$ is shown at the top of Figure 9. This stress, due to the torque, must be superimposed on the stress, shown at the bottom of Figure 9, resulting from the other loads. Doing so indicated that the teeth would not shear off.

V. Structural Integrity Test

In a structural integrity test of the sabot package, two ramjets were fired at $V_r=1325 \text{ m/s}$, 15% below the design velocity. Therefore the axial acceleration was only 85% of the design acceleration. They were fired from a standard one-in-18 twist 105mm gun tube. Therefore the centrifugal load was only 2/3 of that used in designing the package. Even so, several problems were discovered that required modifications to the design.

Despite predictions to the contrary, the sabot petals did indeed engrave. This was a serious problem since the petals were then able to open up while in the bore and thus failed to support the ramjet laterally, resulting in balloting and great aerodynamic jump of the projectile.

The engraving had not occurred as a result of the aluminum yielding into the rifling. Recovered sabot petals showed that the aluminum had actually been eroded and burned away as the petals traveled down the gun bore and spun out against the tube wall. In addition to allowing the petals to rifle, this abrasion also was causing unacceptable gun barrel wear. The petals also had ripped apart once they were unrestrained by the gun tube and were free to spin about their own centers of gravity.

A pusher, recovered from the structural integrity test, showed that much of the pre-engraved rifling had been eroded away by the gun gases. The rubber obturator failed to provide a good seal of the gun gases. The pre-engraved rifling also was worn from friction. A recovered pusher extension was in such good condition that it was capable of being reused.

The structural integrity test showed that sabot petal engraving was a major problem. Less critical but still of concern was the poor obturation. The launch of the ramjet with so much yaw and jump was unacceptable. Modifications to the design needed to be made.

VI. Design Modifications

The changes to be made to the sabot package, as a result of the structural integrity test, are shown in Figure 10.

1. Sabot Petals

The sabot petals are to be modified in several ways. The front air scoop will be removed because the spinning petals will easily separate radially from the ramjet. For the projectiles which will be fired from the smooth tube, the scoop will remain. The flare proved to be stronger than expected. For this reason, the middle support (Figure 2.) will also be eliminated. A benefit resulting from these changes is a weight reduction in the petals, which will lessen their inertial load.

A suggested solution to the engraving problem was to plate the aluminum petals with chrome which would be much more resistant to ablation. However, stress analysis showed that the chrome material would not have been able to withstand the inertial loading. Also, adding the chrome would have required thinning the aluminum petals. With the additional weight of the chrome to carry, the thinner petals would not have been able to withstand the inertial loading.

An alternative will be to hardcoat the petals with a thin layer of aluminum oxide. This should make the petals more resistant to wear. However, the hardcoat on aluminum fins has been known to wear away as they move through the propellant grains in a gun

cartridge. Thus the designer decided not to rely on hardcoat alone to completely solve the problem. In addition to the hardcoat, steel borerider rings will be added in order to prevent the petals from bearing out against the bore.

2. Steel Boreriders

In order to hold the petals together as a unit in the bore, steel boreriders will be shrunk fit at the front and rear of the sabot petals. Steel will not wear away as readily as the aluminum as it presses out against the barrel wall. When the sabot petals exit the barrel, the centrifugal load will break the unrestrained rings and allow the petals to fly away. Of course there is no need for boreriders for the smooth bore.

Considering the steel boreriders as thin vessels with a uniform internal pressure, the hoop stress is:¹¹

$$S_{hoop_{thin}} = \frac{PR}{t} \quad (9)$$

where P is the pressure under the bands due to the centrifugal force (Equation (4)) on the sabot petals, t is the ring thickness, and R is the mean radius of the ring. Out of the bore, the hoop stress for the lowest spin case (1-in-25) must be great enough to break the rings. 1.27mm thick rings, made of AISI 1020 steel (Yield Strength = 207 MPa), should break because the hoop stress computed by Equation (9) is well above the material strength. The rings will be notched in line with the three petals to ensure a symmetric break up into thirds.

A finite-element model of the petals and borerider rings was made using solid 3D elements. Figure 11 shows the displacement of the unrestrained petals and the stress in a borerider at a spin rate of 7,850 rad/s. With stress levels greater than 25 times the yield strength of AISI 1020 steel, the rings will most assuredly break. The FE model also showed that the spinning, unrestrained sabot petals are highly stressed and should fail. In the test firings, upon exiting the gun bore, the petals did indeed break up. The displacement of the petals indicates that they will press out against the gun wall even though they are restrained by the front and rear boreriders. Even if the hardcoating allows some erosion to occur at the middle section of the petals, the front support and flare should still laterally support the ramjet because they are under the borerider.

For this reason, it is of greater concern whether or not the rings will break in the bore. To model this situation, the centrifugal force computed by Equation (4) was applied as a bearing pressure to one-third the outer surface of the petals and boreriders simulating the reaction force from the gun barrel lands. This effectively restrained the petals under the centrifugal load (Figure 12.) The resulting stress in the rings is below the yield point indicating that the rings will not break in the bore.

3. Copper Rotating Band

The erosion of the pre-engraved rifling occurred below the design velocity and spin rate. At the design velocity and higher spin rates, the aluminum rifling might be completely

eroded away. Therefore a solid copper rotating band, which should better withstand the gun gases and also help provide obturation, will be used. The nominal dimensions of the copper rotating band were obtained from the rotating band of another 105mm projectile.

a. Shrink Fit

A copper rotating band is to be shrunk-fit onto the aluminum pusher. The allowable interference between the band and the pusher was determined from stress considerations in the band. An examination of Lamé's equations for internal pressure in thick-walled cylinders shows the maximum stress to be the tangential or hoop stress, $S_{hoop_{thick}}$, at the inner surface and is determined by: ¹²

$$S_{hoop_{thick}} = P \frac{(R_o^2 + R_i^2)}{(R_o^2 - R_i^2)} \quad (10)$$

where:

- P = radial pressure between members
- R_i = inner radius
- R_o = outer radius

For ductile materials such as copper, the property that is used as a design criterion is the yield strength.¹² In thick-walled cylinders, with no shock loading present, such as in a shrink fit, a working stress of 85% of the yield stress is considered satisfactory since the material at the inner surface may flow slightly and readjust the stress distribution without causing failure.¹³ The radial pressure between the members is obtained from Equation (10) by using 85% of the yield strength for SAE 660 brass (97 MPa) for the maximum allowable hoop stress.

The rotating band will be shrunk fit onto the pusher. The total shrinkage allowance, δ , for a hub on a solid shaft is obtained from:¹³

$$\delta = 2R_i P \left[\frac{1}{E_h} \left(\frac{1 + \left(\frac{R_i}{R_o}\right)^2}{1 - \left(\frac{R_i}{R_o}\right)^2} + \nu_h \right) + \frac{1 - \nu_s}{E_s} \right] \quad (11)$$

where:

- E_s = Modulus of Elasticity for the shaft
- E_h = Modulus of Elasticity for the hub
- ν_s = Poisson's Ratio for the shaft
- ν_h = Poisson's Ratio for the hub

b. Engraving Force

A rotating band must be a relatively soft, malleable material that will easily yield, and thus engage, into the rifling. The engraving force on the rotating band was examined by constructing the FE model shown in Figure 13. The band was fixed where it will engage

the rifling, and the base pressure was applied. The radial pressure between the members found by Equation (10) also was applied. The stress in the band is shown in Figure 13. It most certainly will yield.

To check the additional loading on the pusher due to the engraving force, the band was restrained with boundary elements at the band and pusher interface. The resulting reaction forces were used to estimate an additional stress on the pusher of .17 of the yield stress for 7075-T6 aluminum. Even with this, the stress is still below the yield stress in the pusher.

VII. Summary and Conclusions

The methods utilized in designing the sabot package consisted of a mixture of analytical calculations and finite-element analyses. An attempt was made to verify each method with the other, with FE analysis proving the most valuable. The model was deliberately over-designed by overestimating the worst possible loading conditions. The problems discovered in the structural integrity test resulted not from a calculation or FE modeling mistake but rather from an engineering misassumption, i.e., a failure to anticipate the wear and erosion of the aluminum petals during the launch cycle. The basic integrity of the design has been demonstrated and the design changes made will result in an improved launch capability for the 60mm Flared Ramjet.

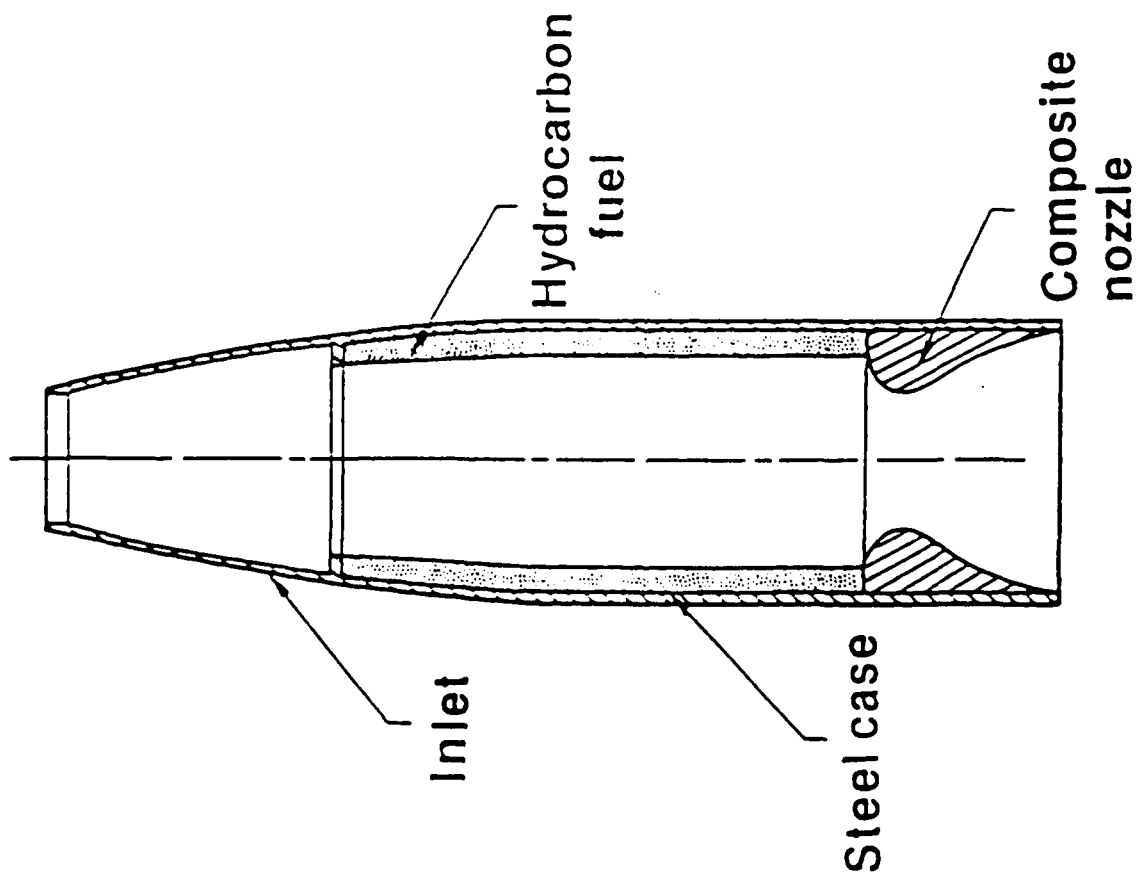


Figure 1. Basic Solid Fuel Ramjet (SFRJ).

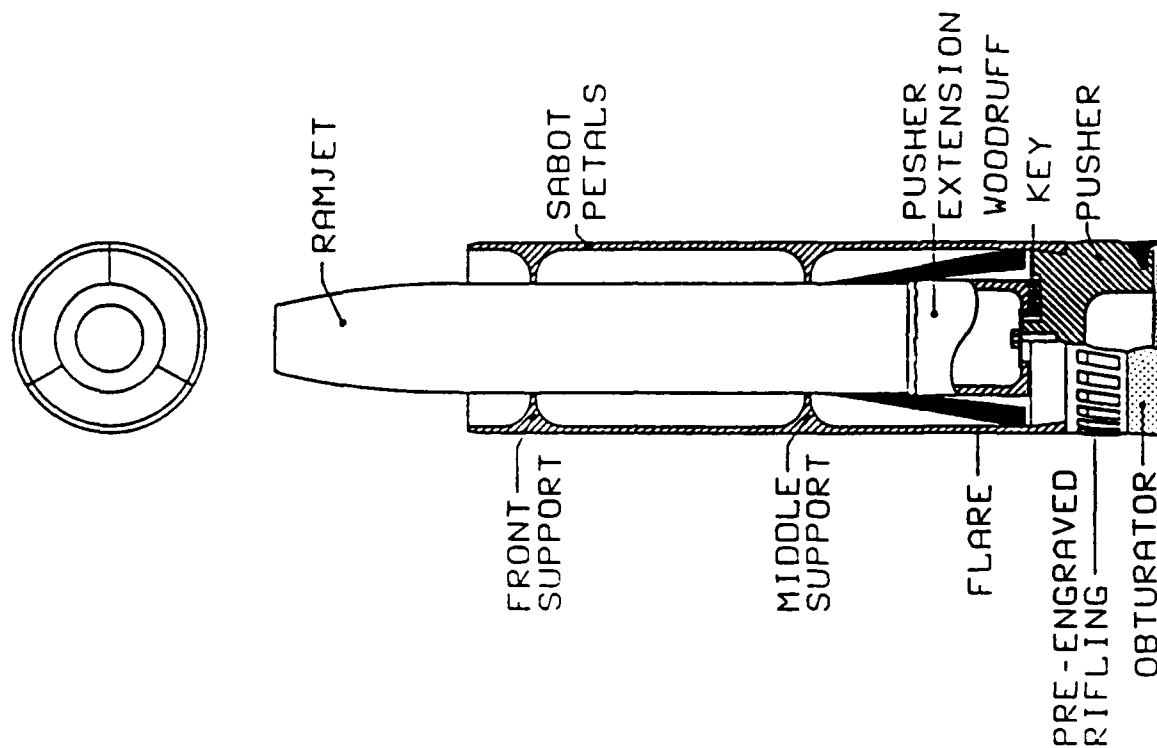


Figure 2. 60mm flared ramjet sabot package.

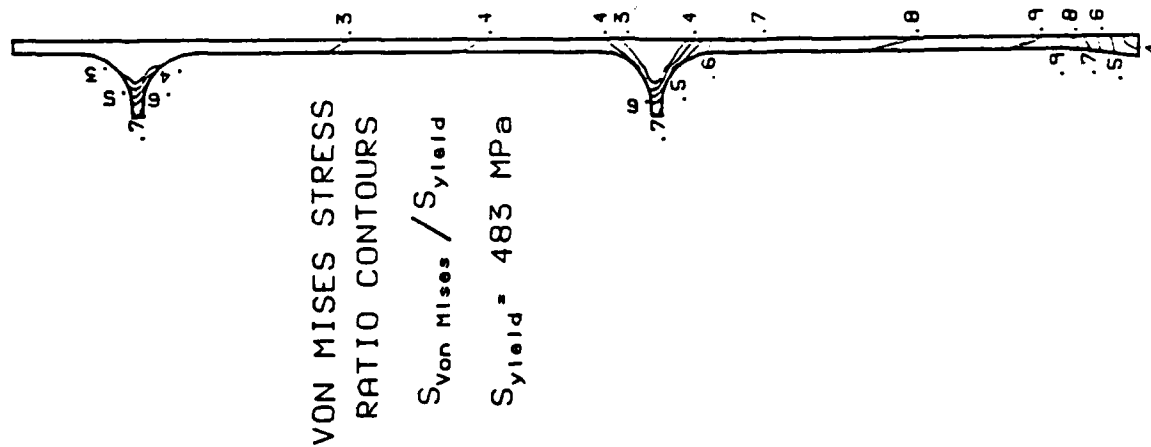


Figure 5. Sabot petal stress contours.

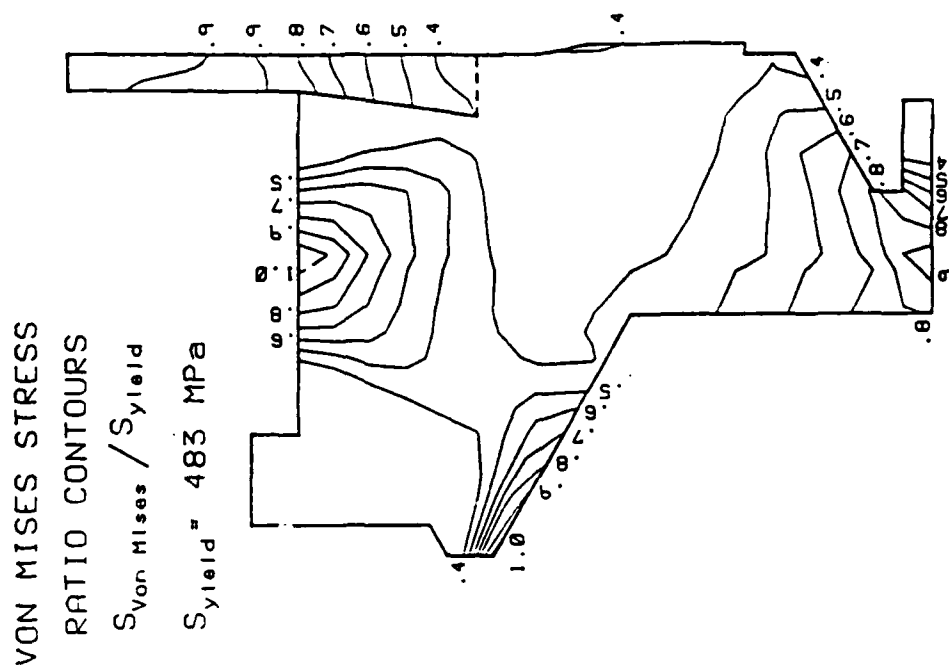


Figure 6. Pusher stress contours.

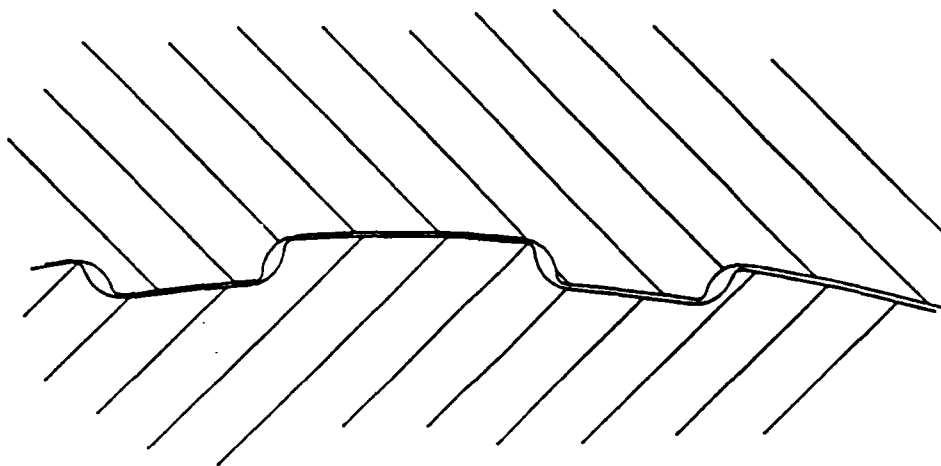


Figure 7. Rifling engagement.

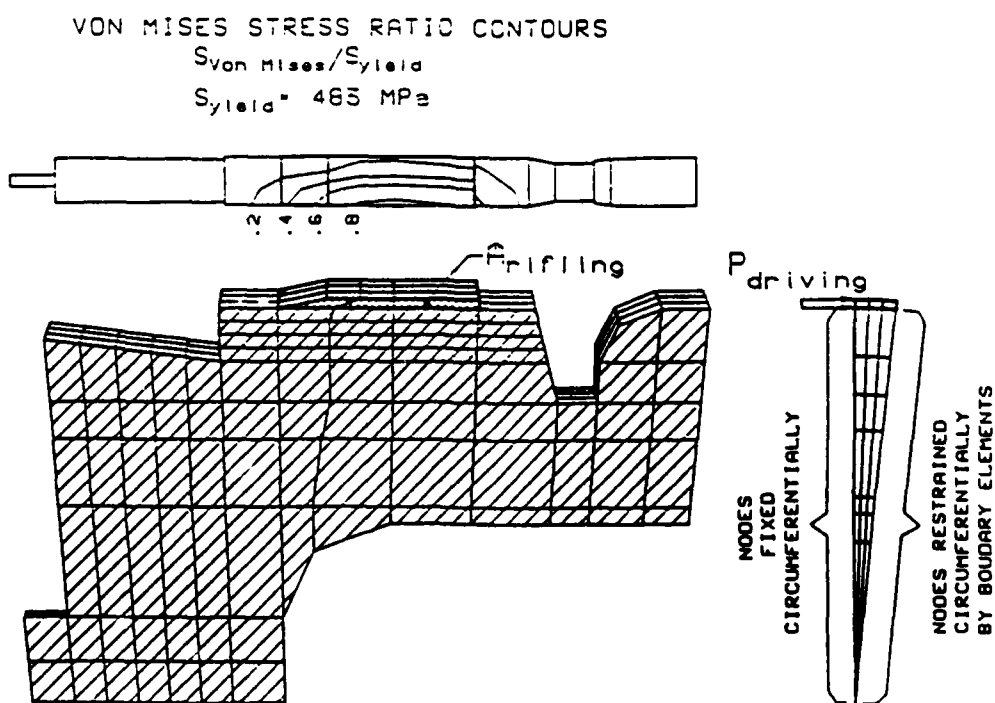
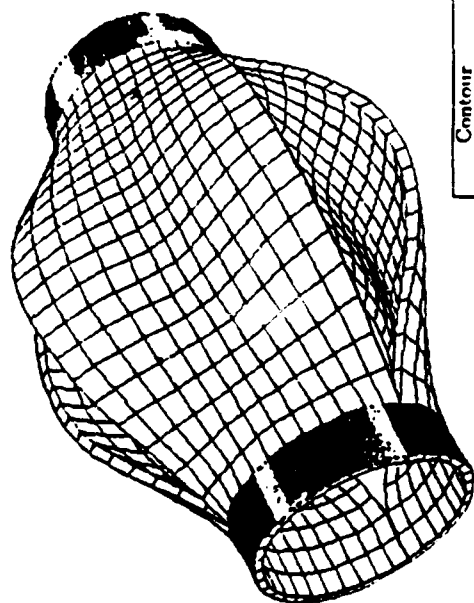


Figure 8. Pre-engraved rifling FE model.



Contour Number	$\frac{S_{\text{max}}}{S_{\text{yield}}}$
1	5
2	15
3	25
$S_{\text{yield}} = 207 \text{ MPa}$	
-	

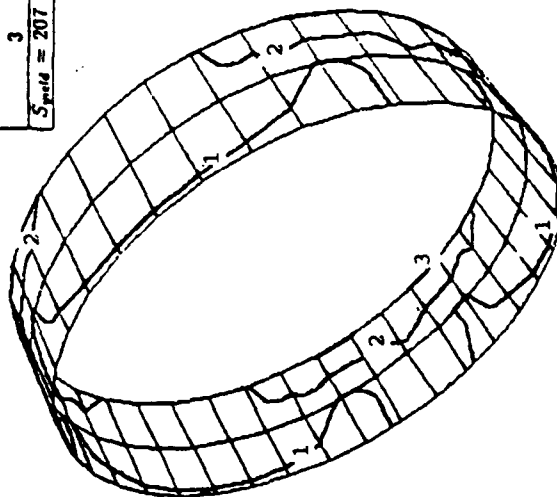
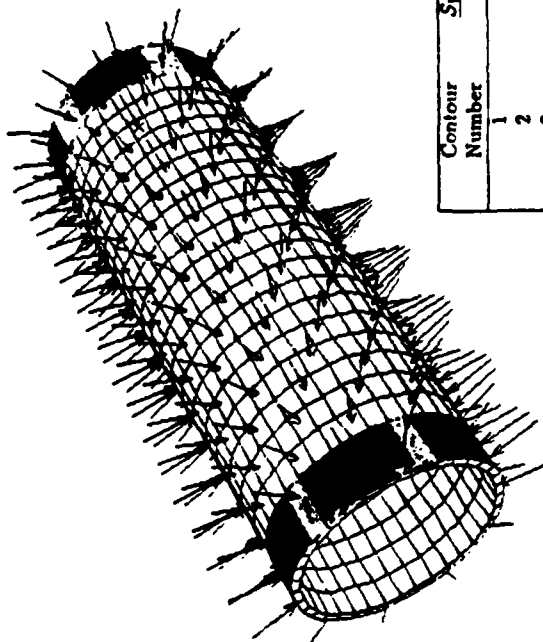


Figure 11. Unrestrained sabot break ring FE model.



Contour Number	$\frac{S_{\text{max}}}{S_{\text{yield}}}$
1	.2
2	.3
3	.4
4	.5
$S_{\text{yield}} = 207 \text{ MPa}$	
-	

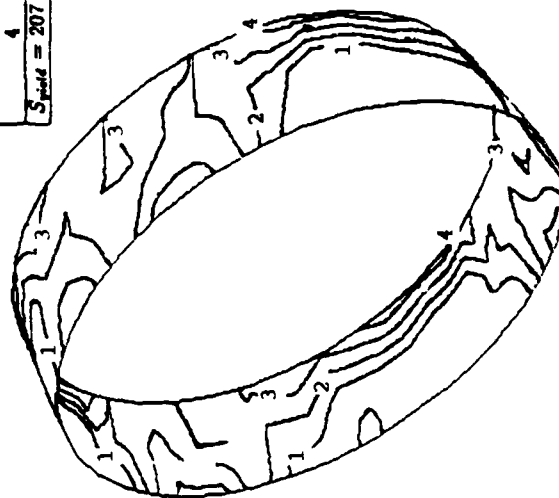
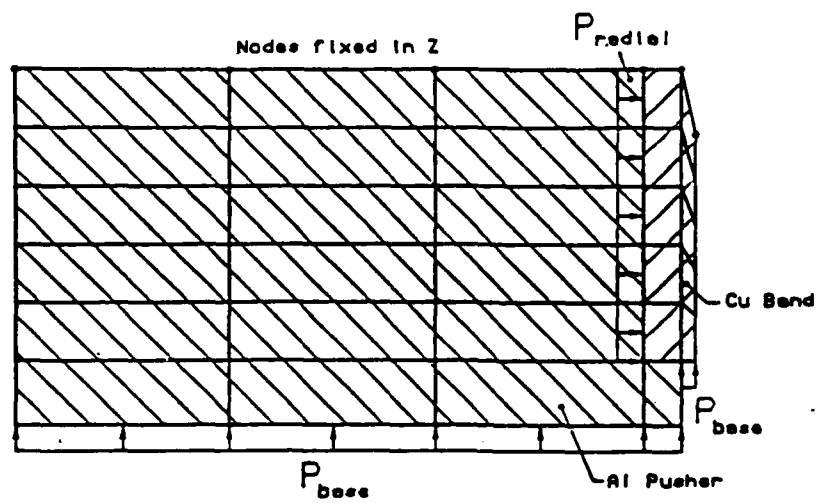


Figure 12. Restrained sabot break ring FE model.



VON MISES STRESS
RATIO CONTOURS

$$S_{Von\ Mises} / S_{yield}$$

$$S_{yield} = 96.5\ MPa$$

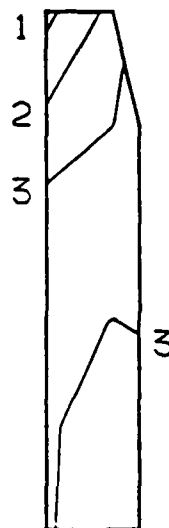


Figure 13. Rotating band FE model.

References

1. Yalamanchili, R.J., Holzman, A.L., "The Effect of Spin on SFRJ Performance", Proceedings of the 1989 Joint Army-Navy-NASA-Air Force Propulsion Meeting, Cleveland, OH., May 1989.
2. Algor, "SUPERSAP - a linear stress analysis program", Algor Interactive Systems, Pittsburg, Pa., 1985.
3. SDRC, "SUPERTAB - a linear stress analysis program", SDRC I-DEAS, Milford, OH., 1985.
4. Pennekamp, R.A., "Finite-Element Analysis of a Sabot for a Finned 60mm Ramjet", BRL-MR-3650, US Army Ballistic Research Laboratory, Aberdeen Proving Ground, Maryland, March 1988. (AD B121011)
5. Crandall, S.H., Dahl, N.C., Lardner, T.J. "An Introduction to Solid Mechanics", McGraw-Hill Book Company, New York, 1972 p.316
6. Sigal, A., Danberg, J.E., "Aerodynamics of Solid Fuel Ramjet Projectiles", BRL-MR-3687, U.S. Army Ballistic Research Laboratory, Aberdeen Proving Ground, Maryland, May 1988. (AD A196755)
7. Drysdale, W.H., "Design of Kinetic Energy Projectiles for Structural Integrity", ARBRL-TR-02365, U.S. Army Ballistic Research Laboratory, Aberdeen Proving Ground, Maryland, September 1981. (AD A105502)
8. Pennekamp, R.A., "Computer Program to Calculate the Physical Properties of One Sabot Petal", BRL-MR-3598, US Army Ballistic Research Laboratory, Aberdeen Proving Ground, Maryland, June 1987. (AD A187222)
9. Sears, F.J., "University Physics, Fifth Edition", Addison-Wesley Publishing Company, Reading, Massachusetts, 1979 p.54
10. Erline, Thomas, "Private Communications", Ballistic Research Laboratory, Interior Ballistics Division, June 89
11. Roark, R. J., "Formulas For Stress And Strain", McGraw-Hill Book Company Inc., New York, 1954 p.247
12. Baumeister, T., "Marks' Standard Handbook for Mechanical Engineers", McGraw-Hill Book Company, New York, 1978 p.5-51
13. Vallance, A., Doughtie, V.L., "Design of Machine Members", McGraw-Hill Book Company, New York, 1943 pp.442,443

List of Symbols

A_{bore}	Bore area
$A_{rifling}$	Driving area of one rifling land
A_{teeth}	Driving area of teeth
a_x	lateral acceleration
a_z	Axial acceleration
d	Depth
dr	Radial travel
dt	Time
dz	Axial travel
E	Modulus of elasticity
FE	Finite-Element
$F_{driving}$	Torque driving force
$F_{centrifugal}$	Centrifugal force
h	Height
I_{zz}	Axial moment of inertia
m	Mass
P	Pressure
P_{base}	Base pressure
$P_{driving}$	Driving pressure
N_{teeth}	Number of driving teeth
R, r	Radial distance

R_{cg}	Radial distance to center of gravity
R_I	Inner radius
R_O	Outer radius
S'	Buckling stress
$S_{hoop,thick}$	Hoop stress, thick ring
$S_{hoop,thin}$	Hoop stress, thin ring
t	Thickness
V_r	Angular velocity
V_z	Axial velocity
δ	Shrinkage allowance
ν	Poisson's ratio
ω	Spin rate
$\dot{\omega}$	Angular acceleration

DISTRIBUTION LIST

<u>No. of Copies</u>	<u>Organization</u>	<u>No. of Copies</u>	<u>Organization</u>
12	Administrator Defense Technical Info Center ATTN: DTIC-DDA Cameron Station Alexandria, VA 22304-6145	1	Director US Army Aviation Research and Technology Activity Ames Research Center Moffett Field, CA 94035-1099
1	HQDA (SARD-TR) Washington, DC 20310-0001	1	Commander US Army Missile Command ATTN: AMSMI-RD-CS-R (DOC) Redstone Arsenal, AL 35898-5010
1	Commander US Army Materiel Command ATTN: AMCDRA-ST 5001 Eisenhower Avenue Alexandria, VA 22333-0001	1	Commander US Army Tank Automotive Command ATTN: AMSTA-TSL (Technical Library) Warren, MI 48397-5000
1	Commander US Army Laboratory Command ATTN: AMSLC-DL Adelphi, MD 20783-1145	1	Director US Army TRADOC Analysis Command ATTN: ATAA-SL White Sands Missile Range NM 88002-5502
2	Commander Armament RD&E Center US Army AMCCOM ATTN: SMCAR-MSI Picatinny Arsenal, NJ 07806-5000	1	Commandant US Army Infantry School ATTN: ATSH-CD-CSO-OR Fort Benning, GA 31905-5660
2	Commander Armament RD&E Center US Army AMCCOM ATTN: SMCAR-TDC Picatinny Arsenal, NJ 07806-5000	1	Air Force Armament Laboratory ATTN: AFATL/DLODL Eglin AFB, FL 32542-5000
1	Director Benet Weapons Laboratory Armament RD&E Center US Army AMCCOM ATTN: SMCAR-LCB-TL Watervliet, NY 12189-4050		<u>Aberdeen Proving Ground</u>
1	Commander US Army Armament, Munitions and Chemical Command ATTN: SMCAR-ESP-L Rock Island, IL 61299-5000		Director, USAMSAA ATTN: AMXSY-D AMXSY-MP, H. Cohen
1	Commander US Army Aviation Systems Command ATTN: AMSAV-DACL 4300 Goodfellow Blvd. St. Louis, MO 63120-1798		Commander, USATECOM ATTN: AMSTE-TO-F
			Commander, CRDEC, AMCCOM ATTN: SMCCR-RSP-A SMCCR-MU SMCCR-MSI

DISTRIBUTION LIST

<u>No. of Copies</u>	<u>Organization</u>	<u>No. of Copies</u>	<u>Organization</u>
1	Commander Armament RD&E Center US Army AMCCOM ATTN: SMCAR-AET-A (R. Kline) Picatinny Arsenal, NJ 07806-5000	1	Director US Army Field Artillery Board ATTN: ATZR-BDW Fort Sill, OK 73503
2	Commander Armament RD&E Center US Army AMCCOM ATTN: SMCAR-FSP-A (F. Scerbo) (J. Bera) Picatinny Arsenal, NJ 07806-5000	1	Commander Defense Advanced Research Projects Agency ATTN: MAJ R. Lundberg 1400 Wilson Blvd. Arlington, VA 22209
1	Commander Armament RD&E Center US Army AMCCOM ATTN: SMCAR-LC Picatinny Arsenal, NJ 07806-5000	1	Aerospace Corporation Aero-Engineering Subdivision ATTN: Walter F. Reddall El Segundo, CA 90245
1	Commander Armament RD&E Center US Army AMCCOM ATTN: SMCAR-CAWS-AM (Mr. DellaTerga) Picatinny Arsenal, NJ 07806-5000	1	Calspan Corporation ATTN: W. Rae P.O. Box 400 Buffalo, NY 14225
1	Commander US Army Missile Command ATTN: AMSMI-RDK (Mr. W. Dahlke) Redstone Arsenal, AL 35898-5010	1	Interferometrics, Inc. ATTN: Mr. R.F. L'Arriva 8150 Leesburg Pike Vienna, VA 22180
1	Commander US Army Dugway Proving Ground ATTN: STEDP-MT (G.C. Travers) Dugway, UT 84022	3	Rockwell International Science Center ATTN: Dr. V. Shankar Dr. S. Chakravarthy Dr. U. Goldberg 1049 Camino Dos Rios P.O. Box 1085 Thousand Oaks, CA 91360
1	Commander US Army Yuma Proving Ground ATTN: STEYP-MTW Yuma, AZ 85365-9103	2	United Technologies Corporation Chemical Systems Division ATTN: Dr. R.O. MacLaren Mr. A.L. Holzman 600 Metcalf Road, P.O. Box 50015 San Jose, CA 95150-0015
1	Commandant US Army Field Artillery School ATTN: ATSF-GD Fort Sill, OK 73503		

USER EVALUATION SHEET/CHANGE OF ADDRESS

This laboratory undertakes a continuing effort to improve the quality of the reports it publishes. Your comments/answers below will aid us in our efforts.

1. Does this report satisfy a need? (Comment on purpose, related project, or other area of interest for which the report will be used.) _____

2. How, specifically, is the report being used? (Information source, design data, procedure, source of ideas, etc.) _____

3. Has the information in this report led to any quantitative savings as far as man-hours or dollars saved, operating costs avoided, or efficiencies achieved, etc? If so, please elaborate. _____

4. General Comments. What do you think should be changed to improve future reports? (Indicate changes to organization, technical content, format, etc.) _____

BRL Report Number _____ Division Symbol _____

Check here if desire to be removed from distribution list. _____

Check here for address change. _____

Current address: Organization _____
Address _____

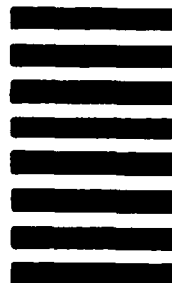
-----FOLD AND TAPE CLOSED-----

Director
U.S. Army Ballistic Research Laboratory
ATTN: SLCBR-DD-T (NEI)
Aberdeen Proving Ground, MD 21005-5066

OFFICIAL BUSINESS



NO POSTAGE
NECESSARY
IF MAILED
IN THE
UNITED STATES



Director
U.S. Army Ballistic Research Laboratory
ATTN: SLCBR-DD-T (NEI)
Aberdeen Proving Ground, MD 21005-9989